Physics – Uspekhi **43** (4) 349 – 364 (2000)

REVIEWS OF TOPICAL PROBLEMS PACS numbers: **71.55.+i**, 71.70.Di, 72.10.Bg, **72.20.–i**

Electron transport in the extreme quantum limit in applied magnetic field

S S Murzin

DOI: 10.1070/PU2000v043n04ABEH000691

Contents

Abstract. The state of the art of electron transport in the extreme quantum limit in magnetic field, when only the lowest Landau subband with one spin orientation is filled, is reviewed for the ionized-impurity scattering case, the one of most experimental interest. The quasi-one-dimensionality of electron motion is taken into account. This results in an essential modification of the conduction processes both along and perpendicular to the magnetic field, in contrast to what was supposed earlier. A reasonably good agreement is obtained with experimental data.

1. Introduction

The theory of conductivity in a quantizing magnetic field was first developed in the 1930s [1, 2] and received a quantum mechanical justification in the 1950s, when conductivity formulas for specific scattering mechanisms were also obtained [3 – 6]. In the limit when the magnetic field is such that only the lowest Landau subband with one spin orientation is filled, it was found that the conductivity does not differ in principle from that for classically strong magnetic fields ($\omega_c\tau \gg 1$, where ω_c is the cyclotron frequency and τ is the transport relaxation time). The conductivity along the magnetic field σ_{zz} obeys the Drude formula

$$\sigma_{zz,0} = \frac{ne^2\tau_0}{m}\,, \tag{1}$$

where n is the electron density, τ_0 is the electron transit time before a backscattering event, and m is the effective mass; the magnetic field is in the z direction. The transverse conductivity

$$\sigma_{xx} = \nu_F e^2 D_{xx} \tag{2}$$

is proportional to the density of states at the Fermi level ν_F and to the transverse (with respect to the magnetic field) diffusion coefficient D_{xx}, which is expressed in terms of the characteristics of microscopic scattering events as [7]

$$D_{xx} = \sum_i \frac{(\Delta x_i)^2}{2\delta t}\,, \tag{3}$$

where the summation runs over the collisions in which the electron participates over a long period of time δt, and Δx_i is the amount by which the average value of the electron's coordinate x changes in the ith collision. In deriving Eqn (3), all the scattering events are assumed to be independent, i.e., in each collision the displacement of an electron in the direction perpendicular to the magnetic field occurs in a random fashion, independently of the previous collisions. The only difference between the extreme quantum limit (EQL) and the case of a classically strong magnetic field is that in the former both the density of states at the Fermi level and the scattering times depend on the magnetic field.

Although the above results have been widely accepted for a long time and can even be found in a number of books and review articles [8 – 12], expressions (1) and (3) have turned out to be fundamentally inapplicable to the quantum limit for the

S S Murzin Institute of Solid State Physics, Russian Academy of Sciences
142432 Chernogolovka, Moscow Region, Russian Federation
Tel. (7-095) 720 49 59 ext. 29-42
Fax (7-096) 576 41 11
E-mail: murzin@issp.ac.ru

Received 13 January 1999
Uspekhi Fizicheskikh Nauk **170** (4) 387 – 402 (2000)
Translated by E G Strel'chenko; edited by S N Gorin

case of ionized-impurity scattering, which is the most important experimentally. The reason is in the quasi-one-dimensional nature of electron motion, i.e., in the fact that the distance an electron travels perpendicular to the magnetic field $r_\perp$ in a time τ_0 is less than the magnetic length $l_m = \sqrt{\hbar c/(eB)}$ and the screening length r_D,

$$r_\perp < l_m < r_D \,. \tag{4}$$

If $r_\perp < r_D$, the independence assumption is not valid for all electron scattering events, making Eqn (3) inapplicable to D_{xx} [13–15]. Scattering perpendicular to the magnetic field can then be considered as a drift motion in two crossed fields, the electric field of an impurity and the external magnetic field [5]. An electron scattered by an impurity reenters the impurity's field many times as it moves quasi-one-dimensionally perpendicular to the magnetic field (Fig. 1), before traveling a distance of order r_D in this direction[1]. Note that since each time the electron drifts the same distance $a \ll r_D$ in about the same direction[2] (see Fig. 1) in the field of the impurity, the electron displacements cannot be considered independent in all scattering acts. Suppose that in the time τ_D an electron needs to travel a distance of order r_D perpendicular to the field, it interacts with P impurities, M times with each. To calculate D_{xx} in this case, one starts by linearly summing the displacements due to a single impurity and only then proceeds to summing the squares of the resulting displacements due to all randomly located impurities,

$$D_{xx} \approx \frac{\sum_{i=1}^{P} \left(\sum_{j=1}^{M} \Delta x_{i,j} \right)^2}{2\tau_D} \approx \frac{a^2}{2\tau_D} \; PM^2 \,, \tag{5}$$

whereas Eqn (3) would give

$$D_{xx} \approx \frac{\sum_{i,j} (\Delta x_{i,j})^2}{2\tau_D} \approx \frac{a^2}{2\tau_D} \; PM \,. \tag{6}$$

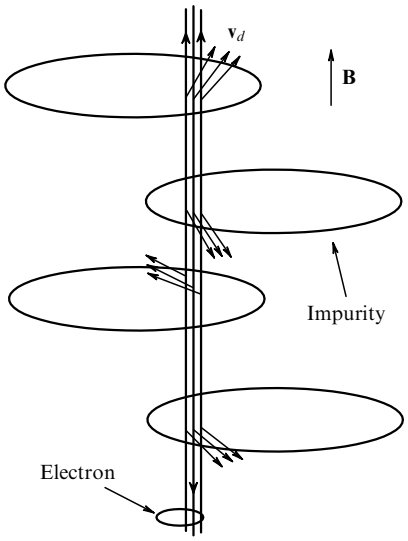

Figure 1. Electron motion in the field of impurities (vertical lines). Impurities are shown schematically as ellipses. The short arrows indicate the electron drift direction.

[1] For one-dimensional diffusion, the number of reentries increases in time as $\sqrt{t}$, whereas in three dimensions the probability of reentry is low.

[2] The importance of accounting for such reentries in calculating the transverse conductivity in nonhomogeneous media was first realized by Dreizin and Dykhne [16, 17].

which is M times smaller. The transverse motion of an electron on a length scale shorter than the screening radius r_D is nondiffusive in character and it is only on length scales longer than r_D that it becomes diffusive (with a step r_D).

For $r_\perp$ below l_m (the characteristic extent of the electron wave function perpendicular to the magnetic field), we approach the one-dimensional situation, in which all electrons are known [18, 19] to be localized due to interference effects. Therefore, the transverse conductivity in the EQL turns out to be much less than its Drude value [15, 20–23]. In the first approximation, neglecting the dependence of the potential on the transverse coordinates x and y, it is valid to consider the electron as localized and to trace the time development of this localized state [15]. First, the transverse components of the nonuniform electric field of the impurities will make it drift perpendicularly to the magnetic field (Fig. 2). Second, its lifetime along the drift path will evidently be finite. Although quasi-one-dimensional (Q-1D) localized effects do not suppress the longitudinal conductivity completely, they reduce it quite significantly.

In addition to the one-electron effects mentioned above, the electron–electron interaction has an important influence on the electron spectrum and transport in the quantum limit. For an electron gas against a uniform positive background in the quantum limit case, theory predicts that charge density waves, Wigner crystals, and other correlated states can be formed as a result of this interaction (see Ref. [24] and references therein). Such effects can perhaps occur in semimetals [25]. This subject, however, is beyond the scope of the present review. In doped semiconductors, the concen-

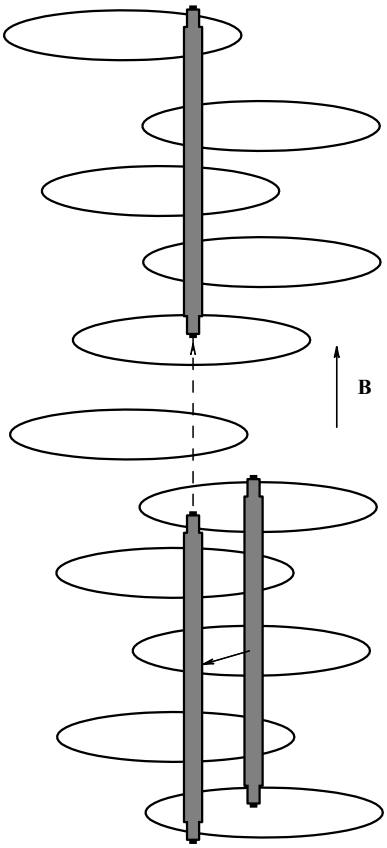

Figure 2. Motion of a quasi-localized electron in the field of impurities. The electron drifts perpendicularly to the magnetic field for some time and then jumps to another drift trajectory.

tration of charged impurities N always exceeds or is equal to the electron density n. Since impurities are distributed randomly, electrons can hardly be expected to form any regular state in the disordered impurity potential. But even in this disordered system the electron–electron interaction significantly affects the density of states and conductivity due to the fact that relative quantum corrections increase with magnetic field [26]. Indeed, in the quantum limit these corrections may become of order unity, implying that the electron–electron interaction may considerably — perhaps radically — affect the properties of a disordered electron system [28, 29].

Another key area that has been revised is the transverse conductivity σ_{xx} of semiconductors in the quantum limit for the case of Boltzmann statistics [30], which differs fundamentally from that of Fermi statistics.

In this review, we consider the longitudinal (σ_{zz}) and transverse (σ_{xx}) conductivity of Fermi and Boltzmann electron gases in semiconductors and semimetals with a simple isotropic spectrum in the magnetic-field quantum limit for the case of predominantly ionized-impurity scattering. The theoretical results will be compared with experiment. The main emphasis will be on semiconductors. Before proceeding with the discussion, however, well-known standard results concerning the behavior of an electron gas in the quantum limit will be summarized first.

2. Fermi (degenerate) electron gas in the quantum limit

2.1 Screening

In the quantum limit, the z component of the electron wave vector at the Fermi level is

$$k_{\mathrm{F}} = 2\pi^2 n l_{\mathrm{m}}^2 \propto \frac{1}{B}\,, \tag{7}$$

the Fermi energy E_{F} as measured relative to the bottom of the lowest subband is

$$E_{\mathrm{F}} = \frac{\hbar^2 k_{\mathrm{F}}^2}{2m} = \frac{2\pi^4\hbar^2 n^2 l_{\mathrm{m}}^4}{m} \propto \frac{1}{B^2}\,, \tag{8}$$

and the density of states is

$$\nu(E) = \frac{1}{(2\pi l_{\mathrm{m}})^2}\,\frac{\sqrt{2m}}{\hbar}\,\frac{1}{\sqrt{E}}\,. \tag{9}$$

The density of states at the Fermi level is $\nu_{\mathrm{F}} \propto B^2$. The Debye screening length is

$$r_{\mathrm{D}} = \left(\frac{4\pi e^2 \nu_{\mathrm{F}}}{\varkappa_0}\right)^{-1/2} = l_{\mathrm{m}}\sqrt{\pi^3 n a_{\mathrm{B}} l_{\mathrm{m}}^2} \propto \frac{1}{B}\,, \tag{10}$$

where $\varkappa_0$ is the dielectric constant of the crystal lattice, and $a_{\mathrm{B}} = \hbar^2\varkappa_0/(me^2)$ is the Bohr radius.

The dielectric constant of a spatially dispersive electron gas in the random phase approximation has the form [31]

$$\varkappa(\mathbf{q}) = \varkappa_0\left(1 + \frac{k_{\mathrm{s}}^2(\mathbf{q})}{q^2}\right), \tag{11}$$

where

$$k_{\mathrm{s}}^2(\mathbf{q}) = \frac{k_{\mathrm{F}}\exp\left(-q_\perp^2 l_{\mathrm{m}}^2/2\right)}{r_{\mathrm{D}}^2 q_z}\ln\left|\frac{2k_{\mathrm{F}} + q_z}{2k_{\mathrm{F}} - q_z}\right|. \tag{12}$$

For $q_\perp \ll l_{\mathrm{m}}^{-1}$ and $q_z \ll k_{\mathrm{F}}$, keeping only two terms in the expansion of the logarithm, and replacing the exponential by 1, we obtain the Fourier transform of the screened potential of an impurity center as [22]

$$V(\mathbf{q}) = \frac{4\pi e}{\varkappa_0\left\{r_{\mathrm{D}}^2 + q_\perp^2 + q_z^2\left[1 + \left(2\sqrt{3}k_{\mathrm{F}} r_{\mathrm{D}}\right)^{-2}\right]\right\}}\,, \tag{13}$$

which means that for $k_{\mathrm{F}} r_{\mathrm{D}} \gg 1$ the screening is of classical (Debye) nature.

In the reverse limit $k_{\mathrm{F}} r_{\mathrm{D}} \ll 1$ (quantum screening), the spatial distribution of the potential is rather complicated. At distances larger than k_z^{-1} from a scattering center along the magnetic field and larger than r_{D} perpendicular to it, the screening length is $1/(2\sqrt{3}k_{\mathrm{F}})$ (i.e., of the order of the electron wavelength) along the field and is about r_{D} perpendicular to the field [22]. For $z = 0$, the potential decreases far more slowly in the direction perpendicular to the magnetic field, namely, at a distance $(r_{\mathrm{D}}/k_{\mathrm{F}})^{1/2}/2 \gg r_{\mathrm{D}}$ [32], due to the contribution of $q_z \sim (k_{\mathrm{F}}/r_{\mathrm{D}})^{1/2}$ to the Fourier integral. This contribution oscillates along the magnetic field and has no effect on the electron scattering [22].

2.2 Scattering

The reciprocal of the backward-scattering time ($1/\tau_0$, with a reversal in the direction of k_z and with a shift of the center of the electron orbit perpendicular to the magnetic field) and the reciprocal of the forward-scattering time ($1/\tau_1$, with an orbit shift, but with no change in k_z) are, in the Born approximation,

$$\begin{aligned}
\frac{1}{\tau_0} &= 8\pi\,\frac{E_{\mathrm{B}}}{\hbar}\,\frac{N l_{\mathrm{m}}^2}{k_{\mathrm{F}}}\int_0^\infty \frac{\exp(-x)}{\left[x + \xi'(x)\right]^2}\,\mathrm{d}x\,,\\
\frac{1}{\tau_1} &= 8\pi\,\frac{E_{\mathrm{B}}}{\hbar}\,\frac{N l_{\mathrm{m}}^2}{k_{\mathrm{F}}}\int_0^\infty \frac{\exp(-x)}{\left[x + \xi''(x)\right]^2}\,\mathrm{d}x\,,
\end{aligned} \tag{14}$$

where $E_{\mathrm{B}} = me^4/2\varkappa_0^2\hbar^2$ is the Bohr energy, and

$$\begin{aligned}
\xi'(x) &= \left[4k_{\mathrm{F}}^2 + r_{\mathrm{D}}^{-2}\exp(-x)\,\frac{\ln(8E_{\mathrm{F}}/\Gamma)}{2}\right]\frac{l_{\mathrm{m}}^2}{2}\,,\\
\xi''(x) &= \exp(-x)\,\frac{l_{\mathrm{m}}^2}{2r_{\mathrm{D}}^2}\,.
\end{aligned} \tag{15}$$

In this result, the screening (see Section 2.1) is better accounted for than in the original works [3, 4] and monograph [8]. The logarithmic singularity in the dielectric function (12) at $q_z = 2k_{\mathrm{F}}$ is removed by including the collisional broadening of electron states [33], whose width is

$$\Gamma = \frac{\hbar}{\tau_0} + \frac{\hbar}{\tau_1}\,. \tag{16}$$

At high temperatures, Γ should be replaced by $\sim 1.5T$, making τ_0 temperature dependent [33]. If $l_{\mathrm{m}} \ll k_{\mathrm{F}}^{-1}, r_{\mathrm{D}}$, then

$$\begin{aligned}
\frac{1}{\tau_0} &= 16\pi\,\frac{E_{\mathrm{B}}}{\hbar}\,\frac{N}{k_{\mathrm{F}}\left[4k_{\mathrm{F}}^2 + r_{\mathrm{D}}^{-2}\ln\left(8E_{\mathrm{F}}/\Gamma\right)/2\right]}\,,\\
\frac{1}{\tau_1} &= 16\pi\,\frac{E_{\mathrm{B}}}{\hbar}\,\frac{N}{k_{\mathrm{F}} r_{\mathrm{D}}^{-2}}\,.
\end{aligned} \tag{17}$$

In semimetals, where impurities are far apart, the condition for the applicability of the Born approximation used in deriving Eqns (14) and (17) is the same as for scattering by a single impurity, i.e., $k_{\mathrm{F}} a_{\mathrm{B}} \sim n a_{\mathrm{B}} l_{\mathrm{m}}^2 > 1$ [37].

In semiconductors, the number of impurities in a volume with characteristic dimensions $1/q_\perp$ and $1/q_z$ is much greater than unity, and the criterion for the application of the Born approximation becomes more stringent, namely

$$U_1 \sim \frac{e^2(Nr_D^3)^{1/2}}{\varkappa_0 r_D} \ll \frac{\hbar v_F}{r_D} \tag{18}$$

in the region of classical screening ($k_F r_D \gg 1$), and

$$U_2 \sim \frac{e^2(Nr_D^2\hat{\lambda}_F)^{1/2}}{\varkappa_0\hat{\lambda}_F} \ll \frac{\hbar v_F}{\hat{\lambda}_F} \sim E_F \tag{19}$$

in the region of quantum screening ($k_F r_D \ll 1$)).

In the above inequalities, U_1 and U_2 are the amplitudes of the fluctuational impurity potential and r_D and $\hat{\lambda}_F = 1/k_F$ are its characteristic lengths. In uncompensated ($N = n$) semiconductors with metallic zero-magnetic-field conductivity, in which the condition $n \gg n_c$ is fulfilled and [34]

$$n_c \approx 0.027 a_B^{-3}\,, \tag{20}$$

both conditions (18) and (19) are always met in fields well below the magnetic field B_{MI} at which the metal–insulator transition occurs.

The nonfulfillment of condition (18) in compensated ($N > n$) semiconductors does not invalidate expressions (14) and (17) for the backward-scattering time τ_0 if a weaker inequality

$$U_1 = \frac{e^2(Nr_D^3)^{1/2}}{\varkappa_0 r_D} \ll E_F \tag{21}$$

is fulfilled, but expressions for the forward-scattering time — and hence expression (16) for Γ — do not apply in this case.

2.3 The region of the quantum limit and the behavior of length characteristics

The transition to the quantum limit occurs in a magnetic field B_{EQL} determined by the condition $E_F \approx \mu_B|g|B = \hbar\omega_c|g^*|/2$, where μ_B is the Bohr magneton, $g^* = gm/m_e$ is the effective g factor, and m_e is the free-electron mass. This field is

$$B_{EQL} \approx 2^{2/3}\pi^{4/3}\,\frac{\hbar c}{e|g^*|}\,n^{2/3}\,. \tag{22}$$

If $g^* \sim 1$, then close to B_{EQL} we have the product $k_F r_D \sim (n^{1/3}a_B)^{1/2} \gg 1$, i.e., the screening is classical. Since k_F and r_D decrease with increasing magnetic field, it follows that at the field

$$B_{QS} = 2\pi^{7/4}\,\frac{\hbar c}{e}\,n^{3/4}a_B^{1/4}\,, \tag{23}$$

for which $2k_F r_D = 1$, a crossover to quantum screening occurs.

In semiconductors, at a still higher field B_{MI}, a metal-insulator transition takes place. For an uncompensated semiconductor, B_{MI} is found from the condition [32, 36]

$$na_B^*(2l_m)^2 \approx \delta, \qquad a_B^* = \frac{a_B}{\ln(a_B/l_m)^2}\,, \tag{24}$$

where a_B^* is the extent, along the magnetic field, of the wave function of an electron bound by an isolated impurity. The extent of the wave function perpendicular to the field is $2l_m$. The exact value of δ is not known. The experimental values of the field B_{MI} for highly doped n-InSb are described by Eqn (24) with $\delta \approx 0.04$ (see Fig. 3, which shows the variation of the fields B_{EQL}, B_{QS}, and B_{MI} with the electron density n for uncompensated n-InSb[3]). Equation (24) is valid only for large a_B/l_m ratios (the solid portion of the $B_{MI}(n)$ curve in Fig. 3). The left, dashed portion is drawn schematically so as to obtain the critical concentration $n_c = 0.027/a_B^3$ in zero magnetic field.

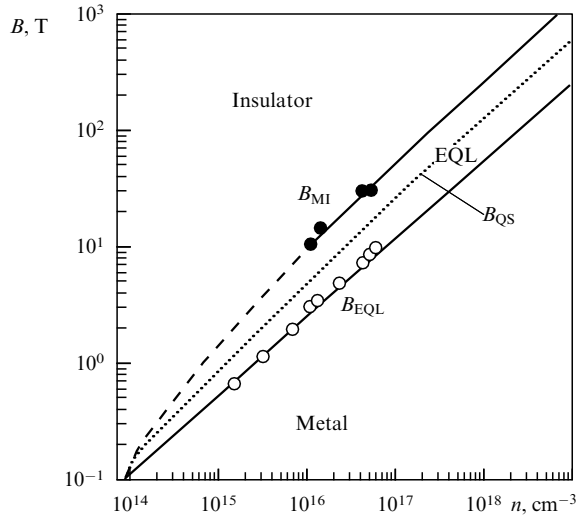

Figure 3. B_{EQL}, B_{QS}, B_{MI} fields as functions of the electron density n for uncompensated n-InSb. Lines, calculation; circles, experimental data.

We now turn to discussing how the characteristics of the electron system behave in highly doped uncompensated semiconductors ($na_B^3 \gg 1$). The Debye screening length (10) is larger than the magnetic length l_m in the region of metallic conductivity because $na_B l_m^2 \gg 1$; it becomes of the same order as the field increases to its metal–insulator transition value B_{MI} (Fig. 4). The electron wavelength at the Fermi level $\hat{\lambda}_F \propto B$ increases with the magnetic field to become of the order of the Bohr radius a_B in the field B_{MI}. The time τ_0 decreases with increasing field in the region of classical screening ($k_F r_D \gg 1$) and then increases in the region where quantum screening dominates ($k_F r_D \ll 1$). The backscattering mean free path of an electron $l_0 = v_F\tau_0$ first decreases with increasing field and becomes $\sim a_B$ in the quantum-screening region. Thus, the region of the quantum limit divides itself into two intervals, (B_{EQL}, B_{QS}) and (B_{QS}, B_{MI}), in which the electron system has substantially different transport properties (see Fig. 4).

It is to be emphasized that as the metal–insulator transition is approached, the mean free path l_0 and the electron wavelength $\hat{\lambda}_F$ both turn out to be of the order of a_B, the localization length along the magnetic field of an electron on an isolated impurity; and the screening length approaches l_m, i.e., becomes of the order of the localization length in the direction perpendicular to the field (see Fig. 4).

[3] The curves in the figure are calculated for the two-band model of Ref. [8] taking into account the dependence of the electron effective mass m on the magnetic field B due to the deviation from the quadratic spectrum. In the region of experimental data, this dependence has little effect on the position of the curves. For large n, its inclusion produces a noticeable but small change in the calculated curves.

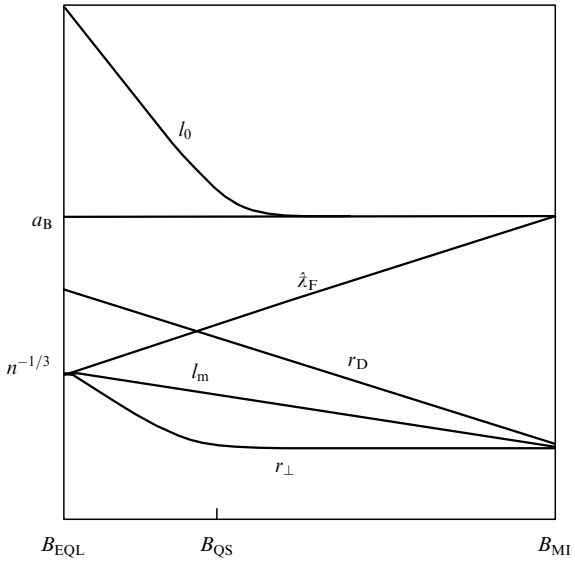

Figure 4. Mean free path l_0, Bohr radius a_B, electron wavelength along the magnetic field $\lambda\!\!\!^{-}_F = 1/k_F$, screening length r_D, magnetic length l_m, and the distance $r_\perp$ an electron travels transversely in a time equal to the backward-scattering time, are plotted as functions of magnetic field for an uncompensated semiconductor with a quadratic spectrum. Logarithmic scale is used.

The value of $r_\perp$ is evaluated using Adams and Holstein's [4] formula $r_\perp = \sqrt{D_{xx}\tau_0}$, to give

$$r_\perp \sim l_m^2\sqrt{4k_F^2 + r_D^{-2}}\,, \tag{25}$$

which is always less than l_m because $l_m k_F = \sqrt{2E_F/(\hbar\omega_c)} < 1$ and $l_m < r_D$. As the magnetic field in the EQL increases, the ratio $r_\perp/l_m$ decreases, reaches a minimum at $k_F r_D \sim 1$, and then increases and becomes of order unity near the metal–insulator transition (see Fig. 4).

3. Transverse conductivity with allowance for scattering correlations

As was noted in the Introduction, in the quantum limit not all scattering events may be treated as independent, and the motion of an electron perpendicular to the magnetic field should be considered diffusive only on scales larger than r_D. The diffusion coefficient in this case can be written in the form $D_{xx} \sim r_D^2/\tau_D$, and the problem reduces to one of finding the time τ_D in which an electron travels a distance of order τ_D perpendicular to the magnetic field. We will estimate τ_D by finding the electron displacement $\Delta X(t)$ as a function of time for $\Delta X(t)$ less than r_D; the time τ_D will be found from the fact that $\Delta X(\tau_D) \approx r_D$.

To obtain $\Delta X(t)$, we make use of the fact that the probability of finding an electron again in the field of a given impurity in time t is

$$W_D \sim \frac{r_D}{\sqrt{D_{zz}t}}\,, \tag{26}$$

where D_{zz} is the coefficient of diffusion along the magnetic field. Consider first the region of classical screening ($k_F r_D \gg 1$), assuming that $E_F \gg U_1$. Since $r_D \gg l_m$, the drift approximation may be applied. For an electron under the electric field of a single impurity $\mathcal{E}_d \sim e/\varkappa_0 r_D^2$, the average transverse drift velocity over the time t is

$$v_d \sim c\,\frac{\mathcal{E}_d}{B}\,W_D = \frac{ce}{\varkappa_0 r_D B(D_{zz}t)^{1/2}} \tag{27}$$

and the corresponding displacement is $\delta x_i(t) \sim v_d t$. The number of impurities with which the electron interacts within the time interval t is

$$P(t) \sim N r_D^2\sqrt{D_{zz}t}\,. \tag{28}$$

Due to the random distribution of the impurities, the square of the total displacement of the electron is

$$\Delta X(t)^2 \sim \delta x_i(t)^2 P(t) \sim \left(\frac{ce}{\varkappa_0 B}\right)^2 N D_{zz}^{-1/2} t^{3/2}\,. \tag{29}$$

Equating the right-hand side of Eqn (29) to r_D^2 yields the time

$$\tau_D \sim \left(\frac{\varkappa_0 r_D B}{ce}\right)^{4/3} N^{-2/3} D_{zz}^{1/3} \tag{30}$$

and the diffusion coefficient

$$D_{xx} \sim \left(\frac{ce}{\varkappa_0 B}\right)^{4/3} N^{2/3} r_D^{2/3} D_{zz}^{-1/3}\,. \tag{31}$$

The transverse conductivity of a degenerate electron gas is [15]

$$\sigma_{xx} = \beta_1\left(\frac{ce^3 v_F}{\varkappa_0 B}\right)^{4/3} N^{2/3} r_D^{2/3}\sigma_{zz}^{-1/3}\,, \tag{32}$$

where β_1 is an unknown numerical factor. Using expressions for the Hall conductivity $\sigma_{xy} = nec/B \gg \sigma_{xx}$, density of states (9) and screening radius (10), the transverse resistivity ($\rho_{xx} = \sigma_{xx}/\sigma_{xy}^2$) can be written in the form

$$\rho_{xx} = \frac{\beta_1}{4^{4/3}\pi^{13/3}}\,\frac{me^{10/3}B^{8/3}}{n^{7/3}c^{8/3}\hbar^4\varkappa_0}\,\rho_{zz}^{1/3}\left(\frac{N}{n}\right)^{2/3}\,. \tag{33}$$

In deriving Eqns (32) and (33), we have neglected contributions to the transverse diffusion (i) from forward-scattering events with impact parameters much less than r_D, and (ii) from backscattering events. If correlations are left out of account, then both types of scattering events make practically the same contribution to the diffusion as the forward-scattering events with impact parameters $\sim r_D$ we considered above. However, in the classical-screening region, correlations act to maximize the contribution to the diffusion from the forward-scattering events with impact parameters $\sim r_D$. The contribution from other scattering events to the transverse motion can be ignored.

In the quantum-screening region, even though $r_D \ll \lambda\!\!\!^{-}_F$, the transverse shift due to forward scattering (with k_z conserved) may again be considered as resulting from drift motion in crossed fields. This conclusion is supported by the fact that the forward-scattering amplitude is the same as for the classical-screening case [see Eqns (14) and (17)]. For backscattering events, whose contribution to the transverse diffusion was not considered above, the correlation length is $r_D\sqrt{2/\ln(8E_F/\Gamma)}$. Therefore, in the quantum-screening region, Eqns (32) and (33) are accurate to within $\sim 1/\ln^p(8E_F/\Gamma)$, where $p > 0$.

Expression (32) is also valid for classically strong magnetic fields, provided the radius of the electron orbit r is less than r_D (then $r_\perp \ll r_D$ automatically). The correlation of scattering events should also be included when calculating the quantum oscillations of the transverse resistivity if $r \ll r_D$.

The above discussion was concerned with the conductivity σ_{xx} of samples whose thickness along the magnetic field was $d \gg \sqrt{D_{zz}\tau_D}$. For $l_0 \ll d \ll \sqrt{D_{zz}\tau_D}$, the value of σ_{xx} depends on d [14].

4. Quasi-one-dimensional localization effects

4.1 Longitudinal conductivity

The influence of localization effects on conductivity was first analyzed by Abrikosov and Ryhzkin [20] on the basis of the scaling hypothesis. For ionized-impurity scattering with $r_D^{-1} \ll k_z \ll l_m^{-1}$, they obtained

$$\sigma_{zz} \sim \sigma_{zz,0}(k_F l_m)^2 \ln\frac{1}{k_F l_m} \propto B^{-6} \ln B\,. \tag{34}$$

An alternative approach is to consider the motion of a quasilocalized electron [15]. As already noted in the Introduction, in the first approximation an electron may be treated as localized, with a localization length $4l_0$ along the magnetic field [19] and l_m perpendicular to it. Taking into account the transverse component of the electric fields of the impurities leads to the drift of the electrons (see Fig. 2). It has been suggested [15, 21, 22] that an electron becomes delocalized when it has traveled far enough perpendicular to the magnetic field for the localization conditions to change [15, 22]; or when, in terms of Berezinskiĭ's model [19], the trajectories of interfering waves encircle an area of order l_m^2 [21] in the plane of the magnetic field. The distance an electron travels parallel to the magnetic field is then l_0, and the longitudinal diffusion coefficient is

$$D_{zz} \sim \frac{l_0^2}{\tau_{dl}}\,, \tag{35}$$

where τ_{dl} is the delocalization time. The results of Refs [15, 21, 22] agree within a logarithmic factor with those of Abrikosov and Ryhzkin, but they also cannot be considered sufficiently well-grounded.

Meshkov [23] takes a more reasonable approach by treating diffusion along the magnetic field as resulting from the jumps that a quasilocalized electron makes from one drift trajectory to another (see Fig. 2). The potential in this model is a smooth nonuniform one with an amplitude U_0/e and a characteristic length $b \gg l_m$, and the electron mean free path along the magnetic field is prescribed and obeys the inequality $l_0 \gg b$. In this case, the drift velocity of a quasilocalized electron along an equipotential line is

$$v_d = c\frac{U_0}{ebB}\,\frac{b}{l_0}\sqrt{\frac{l_0}{b}}\,. \tag{36}$$

The factor b/l_0 accounts for the probability of finding an electron in a region of size b, and $\sqrt{l_0/b}$ results from the summation over various regions in each of which the electron is drifting in various random directions. The projections of the equipotentials of the same energy on the xy plane intersect one another. For a region of size $L > l_0$ along the magnetic field, the average distance between the intersections of one projection with others is $\Delta E/\nabla E$, where $\Delta E = \hbar v_z/L$ is the energy separation in a region of size L in the one-dimensional case, and v_z is the electron velocity along the magnetic field. The rate at which a drifting electron crosses other equipotential lines of the same energy in the projection onto the xy plane is

$$f(L) = v_d\frac{\nabla E}{\Delta E} = \frac{c\nabla E}{eB}\,\frac{\nabla E L}{\hbar v_z} = \frac{l_m^2\nabla E^2}{\hbar^2 v_z}\,L\,. \tag{37}$$

At the point where the projections of the equipotentials of the same energy (a distance z apart along the magnetic field) intersect one another, the energy levels repel one another by an amount equal to the magnitude of the tunneling integral,

$$\Delta(z) = \frac{\hbar}{\tau_0}\exp\left(-\frac{z}{l_0}\right), \tag{38}$$

analogously to the one-dimensional case.

Using Landau and Zener's method for molecular collisions (see Ref. [39], Sect. 90), Meshkov showed that the probability for an electron to hop to another drift path when passing the intersection is

$$W_{1,2} = 1 - \exp\left[-\frac{2\pi\Delta^2(z)}{\hbar^2\left|\mathbf{v}_{d,1}\times\mathbf{v}_{d,2}\right|}\,l_m^2\right], \tag{39}$$

where $\mathbf{v}_{d,1}$ and $\mathbf{v}_{d,2}$ are the electron's drift velocities along the two trajectories under consideration. According to this expression, the transition probability is determined by the relation between $\Delta(z)$ and the energy uncertainty $\delta E = \hbar/\tau_c$ over the time $\tau_c = l_m/v_d$ needed to pass the intersection point. From Eqn (38) and noting that $\Delta(z) \sim \hbar v_d/l_m$, the electron hopping length is

$$z_h = l_0 \ln\frac{l_m}{\tau_0 v_d}\,. \tag{40}$$

The rate of transition to other equipotentials is equal to that of intersections with equipotentials in the regions of size $L = z_h$,

$$\tau_{dl}^{-1} \sim f(z_h) \sim \frac{l_m^2\nabla E^2}{\hbar^2 v_z}\,z_h \sim \frac{\tau_0 v_d^2}{l_m^2}\ln\frac{l_m}{\tau_0 v_d} \sim \tau_0\alpha^2\ln\frac{1}{\alpha}\,. \tag{41}$$

For the above argument to be valid, the parameter

$$\alpha \equiv \frac{\tau_0 v_d}{l_m} \tag{42}$$

must be small. The diffusion coefficient along the magnetic field is

$$D_{zz} \sim \frac{l_0^2}{\tau_0}\alpha^2\ln^3\frac{1}{\alpha}\,, \tag{43}$$

and the conductivity is

$$\sigma_{zz} \sim \sigma_{zz,0}\alpha^2\ln^3\frac{1}{\alpha}\,. \tag{44}$$

For a charged-impurity potential, in the classical-screening region ($k_F r_D \gg 1$) for $b \sim r_D$, we have $U_0 \sim e^2(Nr_D^3/r_D)^{1/2}$, and $\alpha \sim k_F l_m$. Equation (44) differs from Eqn (34) only in the power in the logarithmic factor. In the case of the charged-

impurity potential, since potentials on various scales less than r_D contribute to a comparable extent to the motion of an electron, the actual expression for σ_{zz} may differ from Eqn (44) in having additional logarithmic factors that act to decrease the localization factor.

Under quantum-screening conditions ($k_F r_D \ll 1$), we have $\alpha \sim l_m/r_D$. Then, to within logarithmic factors, the quantity $\sigma_{zz} \propto B^2$ increases with increasing magnetic field [22] because of the increase in $\sigma_{zz,0}$ and α.

4.2 Effect of electron – phonon scattering

Electron – phonon scattering can cause an electron to jump more frequently between the equipotential lines along which it drifts (see Fig. 2), with the result that the longitudinal conductivity increases with temperature[4]. If the electron – phonon scattering time $\tau_0 \ll \tau_{e-ph}(T) \ll \tau_{dl}$ and $T \gg \hbar/\tau_0$, then the longitudinal conductivity assumes the same form as for the one-dimensional case [41]:

$$\sigma_{zz}(T) \sim e^2 \nu_F v_F^2 \, \frac{\tau_0^2}{\tau_{e-ph}(T)} \,. \tag{45}$$

At higher temperatures, where $\tau_{e-ph}(T) \ll \tau_0$, the temperature dependence of σ_{zz} is reversed.

4.3 Transverse conductivity

In the case of classical screening, a quasilocalized electron travels a distance $\sim \hat{\lambda} \ll r_D$ in the transverse direction before jumping to another state. As in the case of no localization, it interacts with any impurity many times also after jumping to another drift trajectory. The procedure that led to Eqns (32) and (33) is applicable in this case as well [15]. Localization effects modify only the probability of finding an electron in the field of an impurity, which circumstance is taken into account through the diffusion coefficient D_{zz}.

In the quantum-screening case ($k_F r_D \ll 1$), the transverse displacement of a quasilocalized electron is $\sim r_D/\ln(r_D/l_m)$ and relations (32) and (33) are accurate to within fractional corrections $\sim 1/\ln(r_D/l_m)$.

Expressions (32) and (33) also remain valid at high temperatures — as long at least as phonon scattering does not contribute importantly to the transverse diffusion. In contrast to the longitudinal conductivity, the transverse conductivity, for which we have

$$\sigma_{xx}(T) \propto \sigma_{zz}^{-1/3}(T) \tag{46}$$

according to Eqn (32), must decrease with increasing temperature in this case. Thus, as the temperature increases, the longitudinal conductivity increases, whereas the transverse conductivity decreases — exactly the opposite to what old theories predict for electron – phonon scattering.

5. Electron – electron interaction

The electron – electron interaction affects conductivity in a number of ways. First, for $T \gtrsim \hbar/\tau_0$, it weakens Q-1D localization effects, with the result that longitudinal conductivity increases with increasing temperature. Murzin [40] has shown that in time τ_0, under the action of the alternate electromagnetic fluctuational field due to electron motions, the phase of an electron with a near-Fermi energy changes (in a random way) by an amount of order unity at a temperature

$$T_\varphi \sim \left(\frac{\hbar \varkappa_0 v_F}{e^2}\right)^{1/3} \frac{\hbar}{\tau_0} \sim \left(\frac{E_F}{E_B}\right)^{1/6} \frac{\hbar}{\tau_0} \,. \tag{47}$$

This means that above this temperature the electrons are delocalized and that the longitudinal conductivity σ_{zz} is described by the Drude formula (1). Note that the relation (32) between the transverse conductivity and longitudinal conductivity is again valid. The main contribution to the phase break comes from fluctuations with $(\omega - v_F K_z) \sim 1/\tau_0$, i.e., from the interaction of a given electron with electrons with close velocities.

The second point is that the electron – electron interaction could affect the probability and the hopping length in Meshkov's model. To clarify the matter, compare the quantity

$$\Delta(z_h) = \frac{\hbar}{\tau_0} \exp\left(-\frac{z_h}{l_0}\right) = \frac{\hbar}{\tau_0}\alpha \tag{48}$$

[see Eqns (38), (40), and (42)] with the Coulomb energy $E_Q \sim e^2/(\varkappa z_h)$, noting, in doing so, that in the quasi-one-dimensional case the dielectric constant at frequencies $1/\tau_{dl} \ll \omega \ll 1/\tau_0$ is [20]

$$\varkappa = \frac{32\zeta(3)}{\pi} \, \frac{e^2}{\varkappa_0 \hbar v_F} \left(\frac{l_0}{2\pi l_m}\right)^2 . \tag{49}$$

It turns out that in uncompensated semiconductors E_Q is always much less than $\Delta(z_h)$ and hence the interaction has no effect on the electron hopping.

Third, at low temperatures $T < \hbar/\tau$, the single-particle density of states (SPDOS) ν^{sp} near the Fermi level and the diagonal components of the conductivity tensor σ_{ii} acquire quantum corrections [26, 27]. In three dimensions, the relative corrections to the SPDOS at the Fermi level ν_F^{sp} and that to σ_{ii} are given by

$$\frac{\delta \nu_F^{sp}}{\nu_F} \sim \frac{\delta \sigma_{ii}}{\sigma_{ii}} \sim -\frac{\lambda(\tau^{-1/2} - T^{1/2})}{\nu_F (D_{xx} D_{yy} D_{zz})^{1/2} \hbar} \,, \tag{50}$$

where λ is the coupling constant of order unity. While in zero magnetic field these corrections are small, $\sim [\hbar/(E_F\tau)]^2$, in a classically strong field they increase by a factor of $(\omega_c\tau)^2$ due to a decrease in the transverse diffusion coefficient, to become

$$\frac{\delta \nu_F^{sp}}{\nu_F} \sim \frac{\delta \sigma_{ii}}{\sigma_{ii}} \sim -\left(\frac{\hbar\omega_c}{E_F}\right)^2 , \tag{51}$$

whereas $\delta\sigma_{xy} = 0$.

When applied formally to the quantum limit in the point-defect scattering case (when Q-1D localization effects are unimportant), the values indicated in Eqn (50) lead to $\delta\sigma_{ii}/\sigma_{ii} \sim -1$. Consequently, the interaction becomes strong, thus invalidating the perturbation theory expression (50). In the case of scattering by ionized impurities, we may attempt to estimate $\delta\sigma_{ii}/\sigma_{ii}$ by using Eqn (50) and taking τ to be equal to the time τ_D it takes an electron to travel a distance r_D perpendicular to the magnetic field (its motion becomes three-dimensional diffusion in this case). Then, noting also that $D_{xx} \sim r_D^2/\tau_D$ and using Eqns (31) and (43), in the case of classical screening ($k_F r_D \gg 1$), we have (to within logarithmic

[4] Temperature T is in energy units throughout.

factors)

$$\frac{\delta\sigma_{ii}}{\sigma_{ii}} \sim -\frac{1}{(k_{\rm F}r_{\rm D})^{4/3}} \propto B^{4/3}\,. \tag{52}$$

In the quantum-screening regions, we obtain $\delta\sigma_{ii}/\sigma_{ii} \sim -1$.

We now turn to discuss, within the framework of current models, how the electron–electron interaction might affect conductivity at low temperatures $T < \hbar/\tau_{\rm D}$. In the classical-screening region, quantum corrections to the conductivity are small and, since electron diffusion is three-dimensional for $t > \tau_{\rm D}$, are proportional to $\sqrt{T}$ in both a zero and a classically strong magnetic field. In the quantum-screening case, two possibilities arise.

1. While the conductivity changes considerably with increasing temperature, it remains metallic at $T = 0$, with $\sigma_{xx},\ \sigma_{xx},\ \sigma_{zz},\ \sigma_{xy} \neq 0$.

2. At $T = 0$, while near the Fermi level the SPDOS $\nu^{\rm sp}$ is small and the electron states are localized, below the Fermi level delocalized states are present (Fig. 5) [28]. In this case, as $T \to 0$, we have

$$\sigma_{xx},\quad \sigma_{yy},\quad \sigma_{zz} \to 0,\quad \sigma_{xy} \to \gamma_{xy}\frac{nec}{B}\,, \tag{53}$$

$$\rho_{xx},\quad \rho_{yy} \to 0,\quad \rho_{zz} \to \infty,\quad \rho_{xy} \to \gamma_{xy}^{-1}\,\frac{B}{nec}\,, \tag{54}$$

where γ_{xy} is independent of temperature. We will call such a state a Hall conductor. The quantities σ_{xy} and ρ_{xy} in this case are not quantized [5]. The possibility of the conductivity and resistivity tensors behaving in this way was also examined by Halperin [45] for a relatively pure system for the case where pinned spin density waves appear.

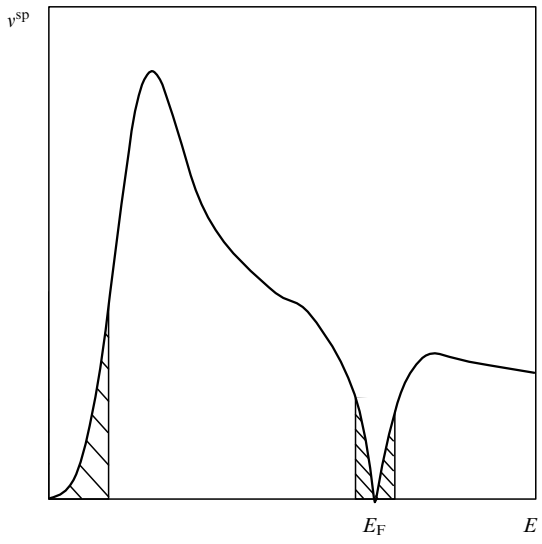

Figure 5. Assumed behavior of the single-particle density of states $\nu^{\rm sp}$ in the quantum limit as a function of energy. The electron localization regions are hatched.

[5] We limit ourselves to thick samples which cannot, at realistic temperatures, satisfy the condition $d < (\hbar D_{zz}/T)^{1/2}$, where d is the sample thickness. In films with a three-dimensional spectrum ($d > l_0$), at low temperatures $T \ll \hbar D_{zz}/d^2$, σ_{xy} and ρ_{xy} show quantization due to the electron–electron interaction [42–44].

At $T < \hbar/\tau_{\rm D}$, σ_{xx} and σ_{zz} should decrease with decreasing temperature as a result of the electron–electron interaction, whereas at higher temperatures a reversed dependence is found for σ_{xx}.

Some aspects of the quantum limit behavior of pure semimetals, related to the fact that the electron density n in these materials exceeds the impurity concentration N, are worth noting here. The interaction of an electron with other electrons increases the velocity of its transverse motion. Although this effect does not contribute to the conductivity directly [8], it may violate the quasi-one-dimensionality condition (4). Two possible consequences of this are, first, that Q-1D localization effects will be suppressed at a temperature $T_{\rm loc}$ below T_φ, and, second, that at a temperature $T_{\rm cor} > T_{\rm loc}$ an electron will not interact repeatedly with impurities. The lower the impurity concentration, the lower the values of $T_{\rm loc}$ and $T_{\rm cor}$. For $T > T_{\rm cor}$, the conductivity can adequately be described by the old theories [3, 4].

6. Boltzmann (nondegenerate) electron gas at $T \ll \hbar\omega_{\rm c}$

6.1 Screening, scattering, and the region of existence of the Boltzmann gas

The Boltzmann electron gas fills only the lowest Landau subband when $T \ll \hbar\omega_{\rm c}$, i.e., in the extreme quantum limit (EQL). Both the component of the characteristic wave vector along the magnetic field $k_T \equiv \hat{\varkappa}_T = \sqrt{2mT}/\hbar$ and the Debye screening length

$$r_{\rm D} = \left(\frac{4\pi e^2 n}{\varkappa_0 T}\right)^{-1/2} \tag{55}$$

are independent of the magnetic field if m and $\varkappa_0$ are.

The Fourier transform of the screened impurity potential is [31, 46]

$$V(\mathbf{q}) = \frac{4\pi e}{\varkappa_0[q_\perp^2 + q_z^2 + \exp(-q_\perp^2 l_{\rm m}^2/2)r_{\rm D}^{-2} I(q_z^2/k_T^2)]}\,, \tag{56}$$

where

$$I(x) = \int_0^1 \exp\left[(t^2 - t)x\right] {\rm d}t = \begin{cases} 1 - \dfrac{x}{6}\,, & x \ll 1\,, \\ \dfrac{2}{x}\,, & x \gg 1\,. \end{cases} \tag{57}$$

For $k_T r_{\rm D} \equiv \sqrt{2}T/(\hbar\omega_0) \gg 1$, the potential is screened classically [$\exp(-q_\perp^2 l_{\rm m}^2/2) \approx 1$] with a radius $r_{\rm D}$. Here,

$$\omega_0 = \sqrt{\frac{4\pi n e^2}{\varkappa_0 m}} \tag{58}$$

is the plasma frequency.

The backward-scattering time $\tau_0(E)$ is given by Eqn (14) with $k_{\rm F}$ replaced by $k_z = \sqrt{2mE}/\hbar$ and with

$$\xi'(x) = \left[4k_z^2 + r_{\rm D}^{-2}\exp(-x) I\left(\frac{4k_z^2}{k_T^2}\right)\right]\frac{l_{\rm m}^2}{2}\,. \tag{59}$$

The condition for the applicability of our treatment is

$$T \gg E_{\rm B,f}\,, \qquad T \gg U_3 \quad \text{or} \quad U_4\,, \tag{60}$$

where

$$U_3 \sim \frac{e^2(Nr_D^3)^{1/2}}{\varkappa_0 r_D} \sim U_0^{3/4} T^{1/4}, \tag{61}$$

$$U_4 \sim \frac{e^2(Nr_D^2 \hat{\lambda}_T)^{1/2}}{\varkappa_0 \hat{\lambda}_T} \sim E_B^{1/4} T^{3/4} \left(\frac{N}{n}\right)^{1/2} \tag{62}$$

are the impurity-potential amplitudes for classical ($T \gg \hbar\omega_0$) and quantum ($T \ll \hbar\omega_0$) screening, respectively; and $E_{B,f}$ is the Bohr energy in a magnetic field. In the large magnetic field limit ($l_m \ll a_B$), we have [35]

$$E_{B,f} = E_B \ln^2 \left(\frac{a_B}{l_m}\right)^2. \tag{63}$$

Over a wide range of fields $B_0 < B < 100B_0$, the dependence of $E_{B,f}$ on B is well approximated by the law

$$E_{B,f} \propto (\hbar\omega_0)^{1/3}, \tag{64}$$

where B_0 is determined from the relation $l_m = a_B$.

With allowance for Eqns (61) and (62), the condition (60) becomes

$$T \gg \max(E_{B,f}, U_{cl}), \qquad T \gg \max(E_{B,f}, U_q), \tag{65}$$

where

$$U_{cl} = e^2 \frac{N^{2/3}}{\varkappa_0 n^{1/3}}, \qquad U_q = E_B \left(\frac{N}{n}\right)^2. \tag{66}$$

The values of U_{cl} and U_q are exactly the activation energies obtained by Shklovskiĭ and Efros [32], implying that the reversal of inequalities (65) leads to dielectric conductivity.

In Figure 6, the phase diagrams of an electron system in the extreme quantum limit are shown. In these, neglecting the magnetic field dependence of m and $\varkappa_0$, only the Bohr energy $E_{B,f}$ and the Fermi energy E_F depend on the field — but then they are independent of the impurity concentration N. If $\hbar\omega_0 \ll E_B$, which is equivalent to $na_B^3 \ll 1$, the region of quantum screening is absent in the diagrams. Since the Fermi energy in the quantum limit, Eqn (8), decreases with increasing field, what was a Fermi electron gas in zero magnetic field becomes a Boltzmann gas in a strong field.

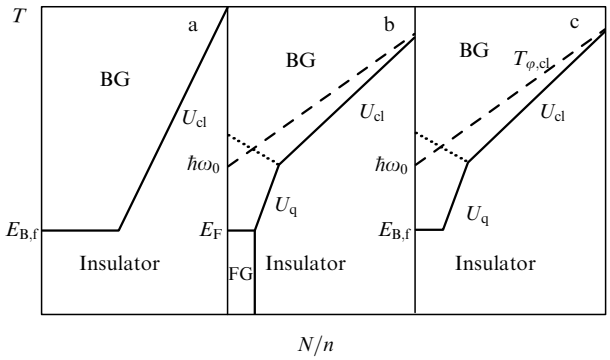

Figure 6. $T - N/n$ diagram of an electron system for (a) $\hbar\omega_0 \ll E_B$, (b) $\hbar\omega_0 \gg E_F \gg E_{B,f}$, and (c) $\hbar\omega_0 \gg E_{B,f} \gg E_F$. The boundaries between these phases (Boltzmann gas (BG), Fermi gas (FG), and insulator) are shown as solid lines. In the region below the dashed line, quasi-one-dimensional effects may affect the conductivity. In the region above the dotted line, the conductivity is described by Eqn (81).

6.2 Quasi-one-dimensional localization effects

In the EQL regime, the condition (4) for an electron to move in one dimension is always satisfied. In uncompensated semiconductors, however, as a result of the electron–electron interaction, localization effects are suppressed even if the electrons obey Fermi statistics. In compensated semiconductors ($n \ll N$), localization effects are possible under certain conditions. Let us determine these conditions.

Unlike for a Fermi gas, the phase break of an electron is not dominated by its interaction with electrons having close velocities. If the electrons obey Boltzmann statistics, the phase break time is equal to the electron–electron scattering time τ_e, which has the order of magnitude

$$\tau_e \sim \tau_1(T) \frac{N}{n}, \tag{67}$$

where τ_1 is given by Eqn (17) with k_F replaced by k_z. The condition for the full suppression of the localization effects is that $\tau_e < \tau_0(E)$.

In the case of classical screening, the ratio of these times is

$$\frac{\tau_e}{\tau_0(E)} \sim \frac{(\hbar\omega_0)^2}{T^{1/2}E^{3/2}} \frac{N}{n}, \tag{68}$$

implying that for electrons with an energy $E \sim T$ the localization effects must be suppressed at temperatures above

$$T_{\varphi,cl} \sim \hbar \left(\frac{Ne^2}{\varkappa_0 m}\right)^{1/2} \sim \hbar\omega_0 \left(\frac{N}{n}\right)^{1/2}. \tag{69}$$

At $T \ll T_{\varphi,cl}$ and $N \gg n$, they can have an appreciable effect on the conductivity.

In the quantum-screening case, the ratio

$$\frac{\tau_e}{\tau_0(E)} \sim \frac{N}{n} \tag{70}$$

depends only on the ratio of electron and impurity concentrations. In uncompensated semiconductors, Q1-D localization effects appear to be of little significance. If $n \ll N$, they should affect the electron transport considerably.

In Fig. 6a, the region of Q1-D localization effects is absent (the line $T = T_{\varphi,cl}$ is in the insulating region). In Fig. 6b and 6c, the line $T = T_{\varphi,cl}$ is shown dashed.

6.3 Longitudinal conductivity

Because in the extreme quantum limit the electron energy distribution takes longer than $\tau_0(T)$ to level off [47], it follows that under conditions where Q1-D localization effects are unimportant, the longitudinal conductivity is

$$\sigma_{zz} = -\int_0^\infty \frac{n(E)e^2\tau_0(E)}{m} \frac{\partial f(E)}{\partial E} \, dE = \int_0^\infty \frac{2e^2\tau_0(E)n}{\sqrt{\pi m}} \frac{E}{T^{3/2}} \exp\left(-\frac{E}{T}\right) dE, \tag{71}$$

where

$$n(E) = \int_0^E \nu(E) \, dE = \frac{1}{(2\pi l_m)^2} \frac{\sqrt{8m}}{\hbar} \sqrt{E}. \tag{72}$$

Here, n is the total electron density in the conduction bond, and $f(E) = A(T)\exp(-E/T)$ is the electron distribution

function, where $A(T)$ is found from the condition

$$\int_0^\infty v(E) f(E)\, \mathrm{d}E = n\,. \tag{73}$$

The longitudinal resistivity $\rho_{zz} = 1/\sigma_{zz}$ increases slowly with the field and saturates in the strong-field limit. In the classical-screening region ($T \gg \hbar\omega_0$), the saturation value is

$$\rho_{zz}^{\infty} = \frac{\pi^{3/2}}{2^{5/2}}\, \frac{e^2 m^{1/2}}{\varkappa_0^2}\, \frac{N}{n}\, T^{-3/2}\,. \tag{74}$$

This is less than the zero-magnetic-field value ρ_0, since small-angle scattering, which contributes appreciably to ρ_0 [3], is absent in this case. In the quantum-screening region, the saturation value is

$$\rho_{zz}^{\infty} = 3.09\, \frac{m^{3/2}}{\hbar^2 \varkappa_0}\, \frac{N}{n^2}\, T^{1/2}\,. \tag{75}$$

In reality, the resistivity does not saturate at a given temperature. First, as a result of the nonparabolic nature of the electron spectrum, the electron effective mass m depends on the field in strong fields [48]. Second, as the field increases, so does the electron–impurity binding energy, and at $E_{\mathrm{B,f}} \sim T$ Eqn (71) does not hold. Beyond that value, ρ_{zz} starts to be governed by an activation mechanism and grows rapidly with the field.

In regions where Q1-D localization is important, the conductivity has not yet been studied.

6.4 Transverse conductivity

The transverse conductivity σ_{xx} of a Boltzmann electron gas in a semiconductor is of a fundamentally different nature from that of a Fermi gas. Upon averaging over energy

$$\sigma_{xx} = -\int_0^\infty e^2 v(E) D_{xx}(E)\, \frac{\partial f}{\partial E}\, \mathrm{d}E = \frac{ne^2}{\sqrt{\pi} T^{3/2}} \int_0^\infty \frac{\exp(-E/T)}{\sqrt{E}}\, D_{xx}(E)\, \mathrm{d}E\,, \tag{76}$$

with the diffusion coefficient (31)

$$D_{xx}(E) \propto D_{zz}(E)^{-1/3}\,, \tag{77}$$

the integral in Eqn (76) diverges as $E \to 0$. One might attempt to estimate σ_{xx} by cutting off the integration, depending on the conditions, at $E = \max(E_{\mathrm{B,f}}, U_{\mathrm{cl}})$ or $E = \max(E_{\mathrm{B,f}}, U_{\mathrm{q}})$, but this does not give a correct result — at least not in the case where the wavelength $\lambdabar_U$ of an electron with an energy U_3 [see Eqn (61)] is much less than the screening radius r_{D}. This condition is satisfied at temperatures

$$T \gg \frac{(\hbar\omega_0)^{6/5}}{E_{\mathrm{B}}^{1/5}} \left(\frac{n}{N}\right)^{2/5}. \tag{78}$$

It turns out that the conductivity in this case is dominated by electrons with small energies

$$E_{\mathrm{c}} < E < U_3\,, \tag{79}$$

where E_{c} is the temperature-dependent mobility threshold (Fig. 7a). When hindered by impenetrable impurity potential hills as they are in their motion along the magnetic field, these electrons can avoid them by drifting in the direction perpendicular to the field (Fig. 7b). While few in number, these electrons are by far more mobile in the perpendicular direction than more energetic electrons because, squeezed between two impurity potential hills, they drift almost unidirectionally until a distance r_{D} is covered. The diffusion coefficient for such electrons is

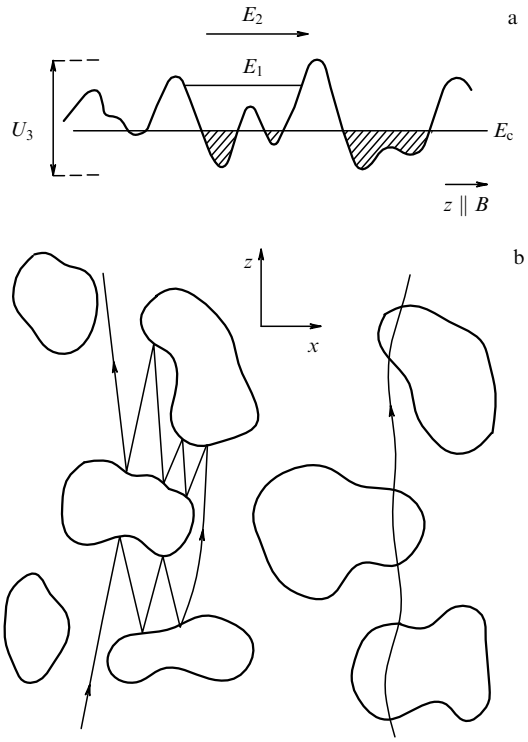

Figure 7. (a) Bending of the bottom of the conduction band. The axis z parallel to the magnetic field is drawn horizontally. The hatched regions lie below the percolation threshold E_{c}. An electron with an energy E_2 moves freely along the magnetic field. An electron with an energy E_1, squeezed along z between two potential maxima, drifts perpendicular to z; (b) motion of electrons with energies E_1 (left) and E_2 (right) in the xz plane. Closed curves are equipotentials bounding the regions inaccessible for an electron with an energy E_1.

$$D_{xx} \sim r_{\mathrm{D}} v_{\mathrm{d}} \sim \frac{cU_3}{eB}\,. \tag{80}$$

Here, $v_{\mathrm{d}} \sim cU_3/eB$ is the electron drift velocity. Since an electron with an energy $E_2 > U_3$ changes its drift direction frequently in a random way as it moves freely parallel to the magnetic field (Fig. 7b), it covers a distance of order r_{D} perpendicular to the field in a much greater time than does an electron with an energy $E_1 < U_3$.

The contribution of low-energy electrons to the conductivity is estimated by inserting $E \sim U_3$ and the diffusion coefficient D_{xx} given by (80) into Eqn (76). Replacing the integration by multiplication by U_3, the transverse conductivity is then [30]

$$\sigma_{xx} \sim \frac{nec}{B} \left(\frac{U_3}{T}\right)^{3/2} \sim \sigma_{xy} \left(\frac{U_{\mathrm{cl}}}{T}\right)^{9/8} \sim \frac{e^{13/4} c n^{5/8} N^{3/4}}{\varkappa_0^{9/8} B T^{9/8}} \tag{81}$$

and, noting that $\sigma_{xx} \gg \sigma_{xy} = nec/B$, the transverse resistivity is found to be

$$\rho_{xx} = \beta_2\, \frac{e^{5/4} N^{3/4} B}{\varkappa_0^{9/8} c n^{11/8} T^{9/8}}\,, \tag{82}$$

where β_2 is an unknown numerical factor.

The region of applicability of Eqns (81) and (82) occupies all the region of existence of the Boltzmann gas in Fig. 6a and lies above the dotted line in Figs 6b and 6c. Below this line, no transverse conductivity has been observed.

For semiconductors with $|g| \ll m_e/m$, there may occur a situation where $\mu_B|g|B \lesssim T \ll \hbar\omega_c$, in which case subbands with two spin orientations are filled. If spin-flip scattering is weak, i.e., electronic intersubband transitions are negligible, and if the electron–electron interaction is unimportant, then each subband may be treated as independent. Unlike the single subband case, the summation over two bands gives rise to an extra factor of $1 + \exp(-\mu_B|g|B/T)$ when physical quantities are calculated. This factor, however, also appears in the normalization condition (73), leading to a reciprocal factor in the coefficient $A(T)$. These factors therefore cancel, leaving us with the single-filled-band results.

7. Experimental results

7.1 Fermi gas

The metallic conductivity region in heavily doped semiconductors in the quantum limit can only be significant if the electron density n is several orders of magnitude greater than the critical concentration n_c for the metal–insulator transition in zero magnetic field. But even then a large difference between the fields B_{EQL} and B_{MI} is not achievable (see Fig. 3), nor can the inequalities (4) (providing that electron motion is quasi-one-dimensional) be made strong. Therefore, the effects discussed above are not very intense. However, they manifest themselves rather distinctly in experiments. The materials most suitable for the experimental study of transport in the quantum limit are heavily doped single crystals of narrow-band n-type semiconductors InSb and InAs, which have a simple isotropic spectrum as well as being high-quality materials.

The first low-temperature magnetoresistance measurements on InSb and InAs date back several decades. The observed magnetic field dependences of the transverse resistivity [49, 50] turned out to be close to that predicted by Adams and Holstein [4], namely, $\rho_{xx} \propto B^p$ with $p \approx 3$, and the resistivity ρ_{xx} was found to depend weakly on temperature in the liquid-helium range (1.5–4.2 K). The general impression was therefore that the problem of quantum-limit transport was by and large resolved. New theoretical studies have stimulated more detailed investigations of the problem. The results are discussed below.

The magnetic-field dependences of the transverse (ρ_{xx}), Hall (ρ_{xy}), and longitudinal (ρ_{zz}) resistivities are illustrated in Figs 8 through 11. Starting from the field B_{EQL}, once the Shubnikov–de Haas oscillations are already over, the transverse resistivity ρ_{xx} increases monotonically with magnetic field (see Fig. 8). The maximum corresponding to where the Fermi level crosses the bottom of the 0^- Landau subband (see Fig. 9) does not show up in the ρ_{zz} (B) dependence because the longitudinal electron velocity at the bottom of the 0^- subband is small and there are no scattering events available to reverse the electron spin from the lowest (0^+) subband to the 0^- subband. Although the theory — both with [22] or without [3] Q1-D localization — predicts that ρ_{zz} first grows in the classical-screening region, then decreases in the quantum-screening region, and then grows again as the metal–insulator transition is approached, nobody has ever seen the decreasing portion, and only a small decrease and a subsequent increase in the derivative $d \ln \rho_{zz}/d \ln B$ has been observed (see Fig. 10). The absence of the decreasing portion is presumably due to the fact that the field B_{QS} is close to B_{MI}, so that the quantum-screening condition $k_F r_D \ll 1$ is not fulfilled.

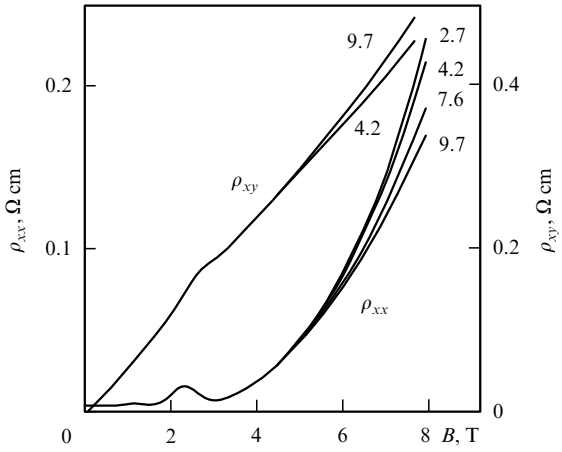

Figure 8. The magnetic field dependence of ρ_{xx} and ρ_{xy} for an n-InSb sample with an electron density of $n = 1.1 \times 10^{16}$ cm^{-3} at various temperatures (shown as labels at the experimental curves). While ρ_{xy} depends markedly on the temperature, the change in σ_{xy} does not exceed 0.7 % [51].

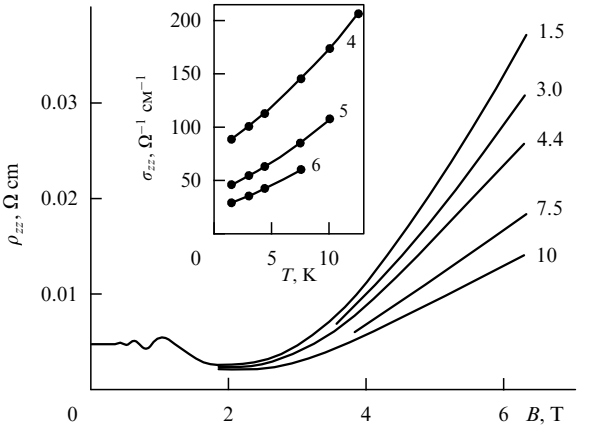

Figure 9. The magnetic field dependence of ρ_{zz} for an n-InSb sample with an electron density of $n = 1.1 \times 10^{16}$ cm^{-3} at various temperatures (shown in units of K at the experimental curves). Inset: the temperature dependence of the longitudinal conductivity $\sigma_{zz} = 1/\rho_{zz}$ at various magnetic fields (shown, in Tesla units, by numbers at the curves).

The relation (33) adequately describes the magnetic-field and electron-density dependences at $T \approx 1.5$ K, when the localization effects have already saturated and electron–electron interactions are not yet important (see below in this section). This was verified by simultaneously plotting the magnetic-field dependences of ρ_{xx} and $C_n B^{8/3} \rho_{zz}^{1/3} m(B)/m$ for a series of uncompensated InSb samples with electron densities in the range $(1-5) \times 10^{16}$ cm^{-3} (see Fig. 11). The factor $m(B)/m$ accounts for the dependence of the electron effective mass on the magnetic field. The coefficients C_n were chosen such that the pair of curves for a particular sample were brought as close as possible to one another. The dependence of C_n on n agrees well with the theoretical prediction $C_n \propto n^{-7/3}$ (Fig. 12). From the experimental data, the numerical coefficient in Eqn (33) is $\beta_1 = 2.1$. The value of

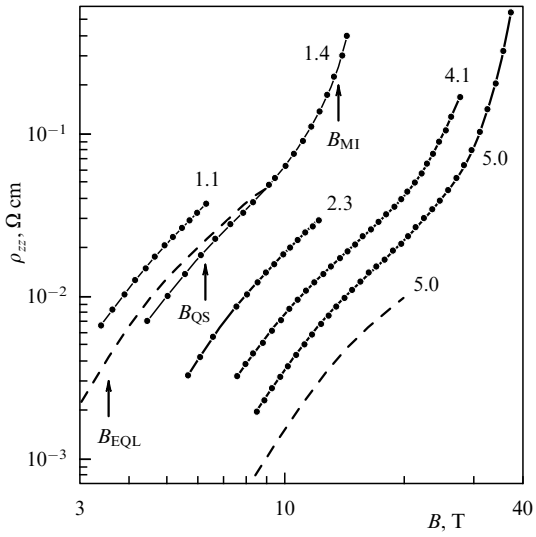

Figure 10. Dependence of ρ_{zz} on B in the quantum limit at $T \approx 1.5$ K for InSb samples with various electron densities. Numbers at the curves indicate n in units of 10^{16} cm^{-3}. Dashed curves are theoretical no-localization results for the minimum (upper curve) and maximum (lower curve) electron densities. The arrows indicate the field values B_{EQL}, B_{QS} and B_{MI} for the sample with $n = 1.4 \times 10^{16}$ cm^{-3} [53].

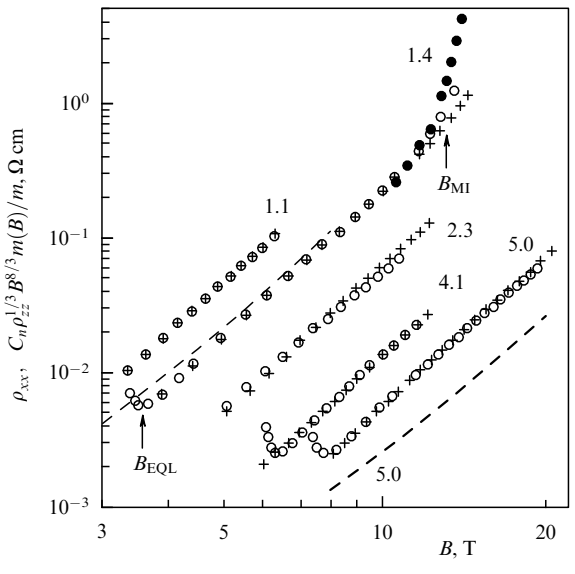

Figure 11. Transverse resistivity ρ_{xx} (○) and $C_nB^{8/3}\rho_{zz}^{1/3}m(B)/m$ (×) for $T \approx 1.5$ K as functions of magnetic field for various samples. Numbers at the curves indicate electron density in units of 10^{16} cm^{-3}. For the sample with $n = 1.4$, the resistivity ρ_{xx} at $T = 80$ mK is also shown to indicate the metal–insulator transition field B_{MI}. Dashed curves are calculated by the theory of Adams and Holstein for samples with minimum (upper curve) and maximum (lower curve) electron densities. The arrows indicate the B_{MI} and B_{EQL} fields for the sample with $n = 1.4$ [53].

the resistivity ρ_{xx} turns out to be 2 to 3 times larger than predicted by Adams and Holstein [4] (see Fig. 11), consistent with the fact that the correlation of scattering events increases the transverse diffusion coefficient D_{xx} and hence the resistivity $\rho_{xx} \approx \sigma_{xx}/\sigma_{xy}^2 \propto D_{xx}$. Fitting the experimental data with a power law $\rho_{xx} \propto B^p$ yields $p = 3.6$, whereas the initial portion of the curve as calculated by Adams–Holstein's formulas is fit well by $\rho_{xx} \propto B^3$.

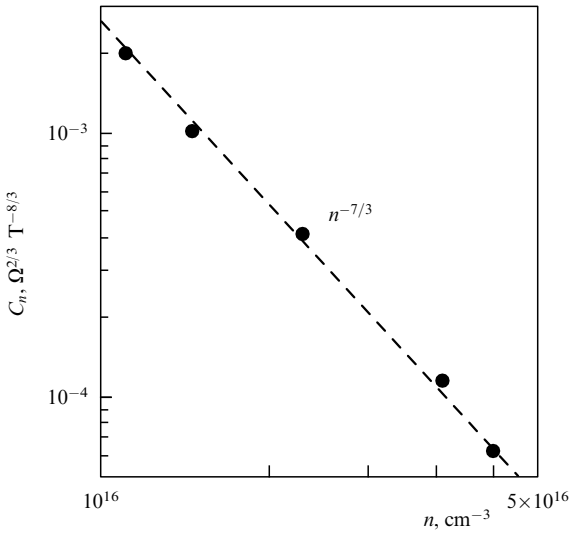

Figure 12. Coefficients C_n obtained from the analysis of the data in Fig. 11 are plotted as functions of electron density. The dashed line corresponds to the dependence $C_n \propto n^{-7/3}$.

The study of the temperature dependence of various components of the resistivity tensor of InSb and InAs in the quantum limit over a wide range of temperatures from 0.05 to 15 K [22, 28, 29, 51, 52] has shown that the diagonal components depend quite sensitively on the temperature (see Figs 8 and 9) whereas the Hall conductivity changes very little with the temperature. The Adams–Holstein theory [4] fails to explain these observations.

The longitudinal resistivity ρ_{zz} decreases with increasing temperature over the entire range of temperatures and magnetic fields [22, 28, 29, 51] (Figs 9 and 13). This can be explained by the suppression of the Q1-D localization effects. However, the electron–phonon scattering is not frequent enough to be of any significance. According to the experi-

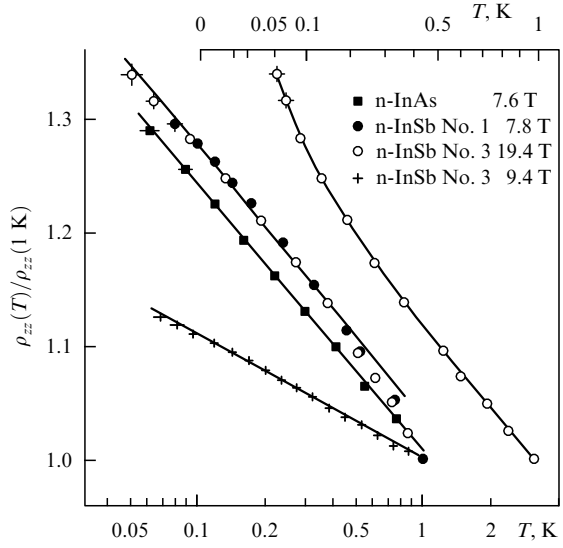

Figure 13. Variation of $\rho_{zz}(T)/\rho_{zz}$ with temperature (plotted on logarithmic scale) for various magnetic fields. Electron density in the InAs sample, $n = 2.7$. Electron density in InSb samples: No. 1, 1.4; No. 3, 5, all in units of 10^{16} cm^{-3}. One of the dependences is on the $T^{1/2}$ scale (upper scale) [29].

mental data, the inelastic scattering time at $T \approx 10$ K must be only a few times less than the elastic scattering time $\tau_0 \sim 10^{-12}-10^{-13}$ s, whereas the electron–phonon scattering time at $T = 10$ K is of order $10^{-9}-10^{-10}$ s. The increase in ρ_{zz} is presumably due to the suppression of the Q1-D localization as a result of the electron phase break caused by electromagnetic fluctuations [40].

The transverse conductivity σ_{xx} and transverse resistivity $\rho_{xx} \approx \sigma_{xx}/\sigma_{xy}^2$ are nonmonotonic functions of temperature in the quantum limit (Figs 14, 15). As the temperature is lowered, σ_{xx} first increases, with the relation (46) holding over certain magnetic field and temperature intervals (see Fig. 14). From the temperature dependence of the conductivity of InSb, the coefficient $\beta_1 \approx 2$ in Eqns (32) and (33), which is close to $\beta_1 = 2.1$, a value obtained from the field dependences. At low temperatures (below 1 K), the transverse conductivity, like the longitudinal conductivity, decreases almost logarithmically [29, 52] (see Figs 13 and 15).

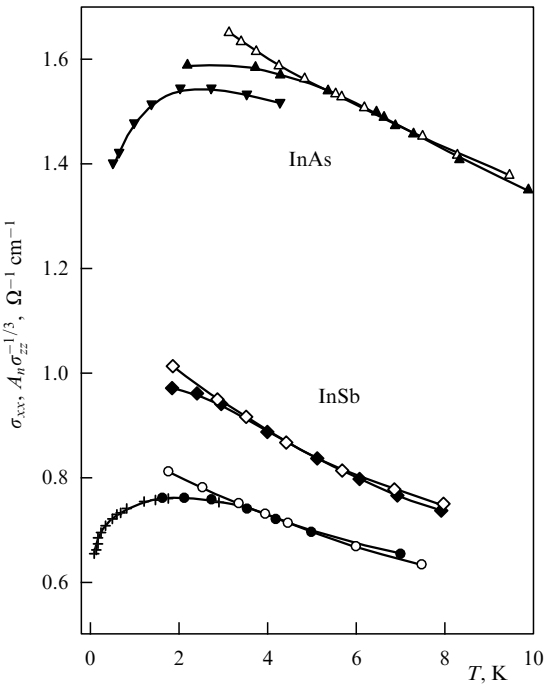

Figure 14. The temperature dependence of the transverse conductivity σ_{xx} (solid symbols and crosses) and $A_n\sigma_{zz}^{-1/3}$ (empty symbols) for a number of InAs and InSb samples for various magnetic fields in the range 6–12 T. Coefficients A_n are selected so as to obtain the best match possible between the curves for one sample in one and the same field in the temperature range 3–6 K [51].

The facts that (i) at low temperatures the diagonal components of the conductivity tensor decrease with decreasing temperature whereas the Hall conductivity remains unchanged, and (ii) the rate of this decrease increases with magnetic field in the classical-screening region (see Figs 13 and 15 and inset in Fig. 15) both agree with the assumption that the temperature dependence of the conductivity is determined by the electron–electron interaction in this case. As the magnetic field approaches its metal–insulator transition value $B_{\rm MI}$, the ratio $\rho_{xx}(1\,{\rm K})/\rho_{xx}(0.08\,{\rm K})$ decreases and becomes less than 1 (inset in Fig. 15). However, the theory of quantum corrections does not explain why the temperature dependences observed are logarithmic rather than of the form

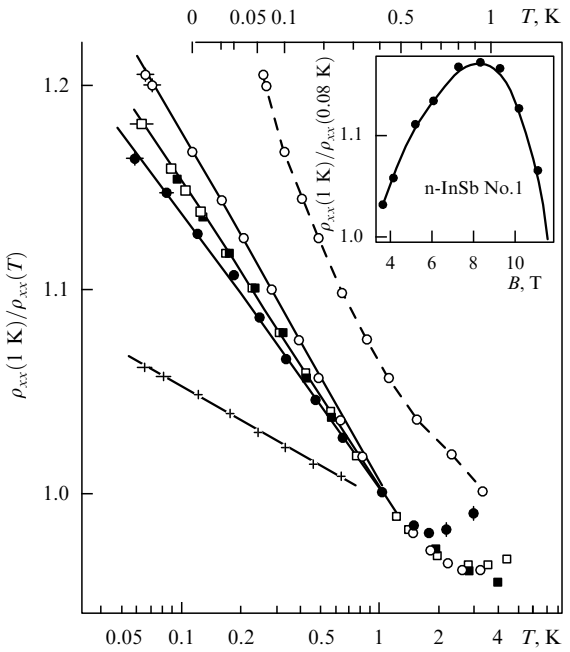

Figure 15. Variation of $\rho_{xx}(1\,{\rm K})/\rho_{xx}(T)$ with the temperature (plotted on a logarithmic scale) for the same samples and same magnetic fields as in Fig. 13. One of the dependences is on a logarithmic scale (upper scale). Inset: the ratio $\rho_{xx}(1\,{\rm K})/\rho_{xx}(0.08\,{\rm K})$ as a function of magnetic field for the n-InSb sample No. 1, with an electron density $n = 1.4 \times 10^{16}$ cm^{-3}.

$A + D\sqrt{T}$ [here, A and D are constants, see Eqn (50)], nor the fact that ρ_{zz} decreases more rapidly than ρ_{xx} as the temperature is lowered.

7.2 Boltzmann gas

The transverse resistivity of the Boltzmann gas in InSb is well described by expression (82) over a wide range of electron concentrations. ρ_{xx} changes approximately linearly with magnetic field (Fig. 16), and $\rho_{xx} \propto T^{-9/8}$ in the temperature range 20–80 K (Fig. 17). For a given temperature and field, $\rho_{xx}/N^{3/4} \propto n^{-11/8}$ (Fig. 18) according to Eqn (82). The experimentally determined numerical factor β_2 in Eqn (82) is 0.3.

The behavior of the longitudinal resistivity of the Boltzmann electron gas in InSb at an electron density of

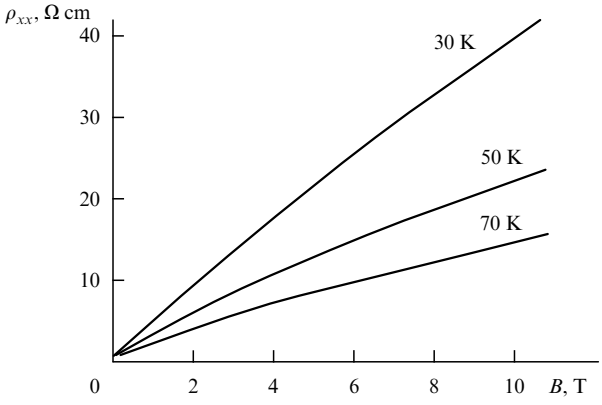

Figure 16. Magnetic field dependence of the transverse resistivity ρ_{xx} for the n-InSb sample with an electron density $n = 3.6 \times 10^{13}$ cm^{-3} at 30, 50, and 70 K [30].

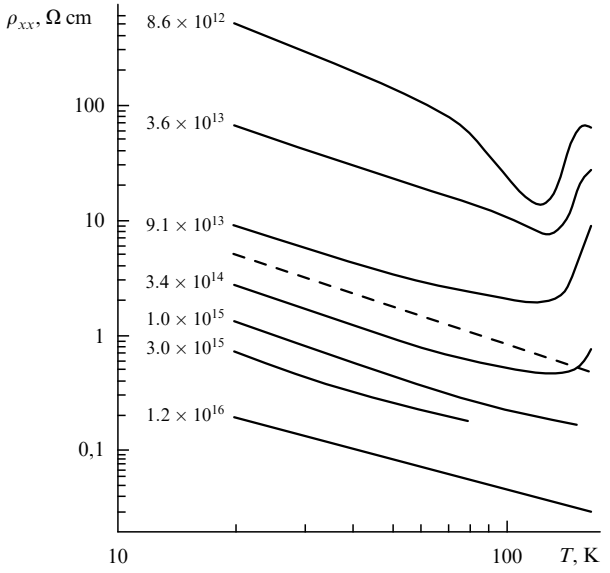

Figure 17. Temperature dependence of the transverse resistivity ρ_{xx} for various samples in a magnetic field of 11 T. The numbers at the curves indicate the electron density n in cm^{-3}. The dashed straight line has a slope corresponding to the dependence $\rho_{xx} \propto T^{-9/8}$ [30].

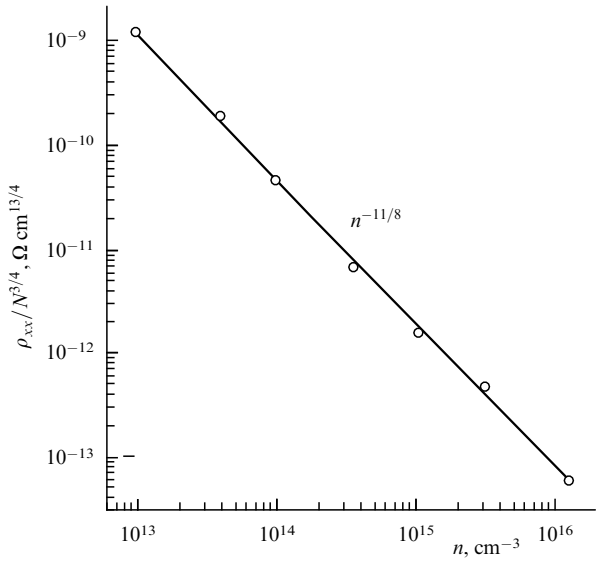

Figure 18. $\rho_{xx}/N^{3/4}$ plotted as a function of electron density from the results for various samples in a field of 11 T at 50 K. The slope of the straight line corresponds to the dependence $\rho_{xx}/N^{3/4} \propto n^{-11/8}$ [30].

$n = 10^{15}\,cm^{-1}$ agrees rather well with theoretical predictions. On passage to the extreme quantum limit, it first drops due to the suppression of small-angle scattering and then depends only slightly on the magnetic field (Fig. 19). Although the rate of the drop should increase with decreasing electron density n as a result of the increased screening length, in reality it decreases and at low enough n the magnetoresistivity becomes positive (Fig. 19). At about $10^{13}\,cm^{-3}$, the discrepancy between experiment and theory is as much as 40 times for $B = 11$ T (Fig. 20) — too much to be attributed to the Q1-D localization effects described above.

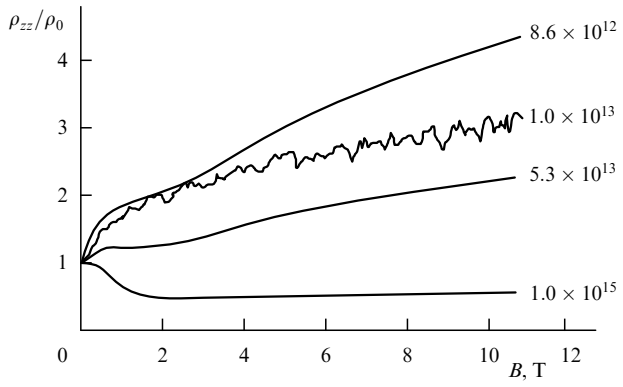

Figure 19. Magnetic field dependence of the longitudinal resistivity ρ_{zz} for various electron density values (indicated at curves) at $T = 30$ K. The curve with noise is for measurements at a high frequency (600 MHz), the remaining curves are for a low frequency (30 Hz) [54].

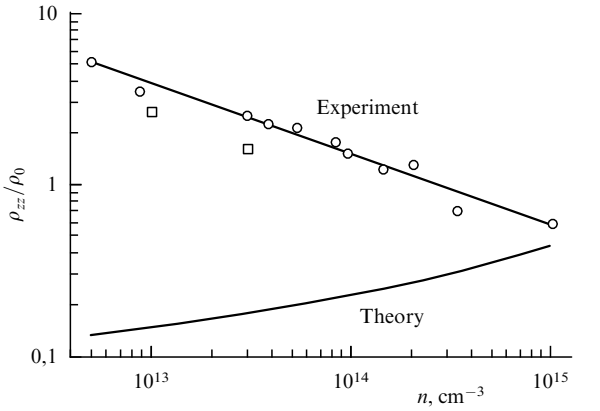

Figure 20. Longitudinal resistivity ρ_{zz}/ρ_0 normalized to the zero-magnetic-field value ρ_0 as afunction of electron density n in a field of 6.3 T at $T = 30$ K [54].

8. Conclusion

The present work reviews the theoretical predictions of and experimental evidence for the fact that quasi-one-dimensional localization effects influence the conductivity in the quantum limit with respect to the magnetic field. It would be an illusion, though, to think that the problem is fully resolved. Although theoretical results agree to within logarithmic or numerical factors, none of them is rigorous. Nor the experimental data do anything more than simply confirm that these effects do indeed manifest themselves — and on more or less the scale predicted.

The transverse conductivity formula (32), allowing for repeated electron – impurity interactions, appears to be valid in the classical-screening regime. In the quantum-screening region, corrections to the right-hand side of this expression are small, $\sim 1/\ln^p(r_D/l_m)$. Although Eqn (32) agrees with experimental data, it is worth remarking that, due to the small difference between the field values B_{MI} and B_{EQL}, it is only over limited intervals of magnetic field and temperature that this equation applies.

As regards the question how the electron – electron interaction affects the conductivity, there has been evidence to confirm the assumption that the diagonal conductivity

tensor components σ_{xx} and σ_{zz} decrease considerably with increasing temperature, whereas the Hall conductivity σ_{xy} does not change. Surprisingly, even though the electron diffusion is three-dimensional in nature, σ_{xx} and σ_{zz}, rather than obeying an $A + D\sqrt{T}$ law, were found to be nearly logarithmic functions of temperature, σ_{zz} varying more rapidly than σ_{xx}. These facts require explanation. It is possible that the logarithmic behavior is due to the fact that in the quantum limit there are only four independent degrees of freedom in phase space (namely, $y, z, k_y = -x_0/l_m^2, k_z$ if one employs the Landau gage [39]) instead of six (x, y, z, k_x, k_y, and k_z).

The most interesting and as yet unanswered question is whether an electron system in the quantum limit is a metal or a Hall conductor (ρ_{xx}, $\rho_{yy} \to 0$, $\rho_{zz} \to \infty$, $\rho_{xy} \to$ const for $T \to 0$). Such a state is, to some extent, similar to the quantum Hall effect in two dimensions, but with ρ_{xy} and σ_{xy} unquantized. A piece of evidence in favor of the Hall conductor is the logarithmic temperature dependence of σ_{xx} and σ_{zz}, because $-\log T \to \infty$ as $T \to 0$. Unfortunately, it has not, as yet, been possible to realize quantum-screening conditions such that the longitudinal resistivity ρ_{zz} would decrease with increasing magnetic field — which is exactly the case where stronger-than-logarithmic temperature dependences of the diagonal components of the resistivity tensor may be hoped for.

The behavior of the longitudinal conductivity of the Boltzmann gas in InSb with a low electron density is another fact which remains to be understood.

We may summarize, then, by saying that, in spite of the considerable recent progress in understanding electron transport in the quantum limit, the full solution of the problem is still a long way off.

Some of the author's works reviewed here were coauthored with A G M Jansen, F A Egorov, N I Golovko, and E Haanappel, to whom the author expresses his sincere gratitude. He is also most grateful to S V Meshkov for communicating some unpublished results, V F Gantmakher and D V Shovkun for their continual encouragement and much advice, and V T Dolgopolov for helpful discussions.

The work was supported by the RFBR–PICS Grant No. 98-02-22037, RFBR Grant No. 98-02-16633, and RFBR–INTAS Grant No. 97-02-71015 (IR 97-76)).

References

1. Titeica S *Ann. Phys.* (Leipzig) **28** 128 (1935)
2. Davydov B I, Pomeranchuk I Ya *Zh. Eksp. Teor. Fiz.* **9** 1924 (1939)
3. Argyres P N, Adams E N *Phys. Rev.* **104** 900 (1956)
4. Adams E N, Holstein T D *Phys. Chem. Solids* **10** 254 (1959)
5. Kubo R, Hasegawa H, Hashitdume N *J. Phys. Soc. Jpn.* **14** 56 (1959)
6. Argyres P N, Roth L M *Phys. Chem. Solids* **12** 89 (1959)
7. Lifshitz E M, Pitaevskiĭ L P *Fizicheskaya Kinetika* (Physical Kinetics) (Moscow: Nauka, 1979) [Translated into English (Oxford: Pergamon Press, 1981)]
8. Gantmakher V F, Levinson I B *Rasseyanie Nositeleĭ Toka v Metallakh i Poluprovodnikakh* (Carrier Scattering in Metals and Semiconductors) (Moscow: Nauka, 1984) [Translated into English (Amsterdam: North-Holland, 1987)]
9. Askerov B M *Elektronnye Yavleniya Perenosa v Poluprovodnikakh* (Electron Transport Phenomena in Semiconductors) (Moscow: Nauka, 1985) [Translated into English (Singapore: World Scientific, 1994)]
10. Kubo R, Miyake S J, Hashitdume N, in *Solid State Phys.* Vol. 17 (Eds F Seitz, D Turnbull) (New York: Acad. Press, 1965) p. 269
11. Roth L M, Argyres P N, in *Semiconductors and Semimetals* Vol. 1 (Eds R K Willardson, A C Beer) (New York: Acad. Press, 1966)
12. Hajdu J, Landwehr G, in *Topics Appl. Phys.* Vol. 57 (Ed. F Herlach) (Berlin: Springer, 1985) p. 17
13. Murzin S S *Pis'ma Zh. Eksp. Teor. Fiz.* **39** 567 (1984) [*JETP Lett.* **39** 695 (1984)]
14. Polyakov D G *Zh. Eksp. Teor. Fiz.* **90** 546 (1986) [*Sov. Phys. JETP* **63** 317 (1986)]
15. Murzin S S *Pis'ma Zh. Eksp. Teor. Fiz.* **45** 228 (1987) [*JETP Lett.* **45** 283 (1987)]
16. Dreĭzin Yu A, Dykhne A M *Zh. Eksp. Teor. Fiz.* **63** 242 (1972) [*Sov. Phys. JETP* **36** 127 (1973)]
17. Dreĭzin Yu A, Dykhne A M, in *Sixth Europ. Conf. on Controlled Fusion and Plasma Phys.* Vol. 1 (Moscow, 1973) p. 147
18. Mott N F, Twose W D *Adv. Phys.* **10** 107 (1979)
19. Berezinskiĭ V L *Zh. Eksp. Teor. Fiz.* **65** 1251 (1973) [*Sov. Phys. JETP* **38** 697 (1974)]
20. Abrikosov A A, Ryzhkin I A *Fiz. Tverd. Tela* (Leningrad) **19** 59 (1977) [*Sov. Phys. Solid State* **19** 33 (1977)]; Abrikosov A A, Ryzhkin I A *Adv. Phys.* **27** 405 (1979)
21. Polyakov D G, in *Proc. 20th Inter. Conf. on Phys. of Semicond.* (Greece, 1990) p. 2321
22. Kosarev V V, Red'ko N A, Belitskiĭ V I *Zh. Eksp. Teor. Fiz.* **100** 492 (1991) [*Sov. Phys. JETP* **73** 270 (1991)]
23. Meshkov S V, Private communication
24. MacDonald A H, Brynt G W *Phys. Rev. Lett.* **58** 515 (1987)
25. Miura N, Shimamoto Y, Nojiri H, in *Proc. 23rd Inter. Conf. on Phys. of Semicond.* (Berlin, 1996) p. 177
26. Al'tshuler B L, Aronov A G *Zh. Eksp. Teor. Fiz.* **77** 968 (1979) [*Sov. Phys. JETP* **50** 968 (1979)]
27. Altshuler B L, Aronov A G, in *Modern Problems in Condensed Matter Sciences* Vol. 10 (Eds V M Agranovich, A A Maradudin) (Amsterdam: North-Holland, 1985)
28. Murzin S S *Pis'ma Zh. Eksp. Teor. Fiz.* **44** 45 (1986) [*JETP Lett.* **44** 56 (1986)]
29. Murzin S S, Jansen A G M *J. Phys.: Condens. Matter* **4** 2201 (1992)
30. Murzin S S, Golovko N I *Pis'ma Zh. Eksp. Teor. Fiz.* **54** 166 (1991) [*JETP Lett.* **54** 551 (1991)]
31. Horing N J *Ann. Phys.* **54** 405 (1969)
32. Shklovskiĭ B I, Efros A L *Zh. Eksp. Teor. Fiz.* **64** 2222 (1973) [*Sov. Phys. JETP* **37** 1154 (1973)]
33. Paulus U, Hajdu J *Solid State Commun.* **20** 687 (1976)
34. Mott N F, Davis E A *Electronic Processes in Non-Crystalline Materials* (Oxford: Clarendon Press, 1971)
35. Shklovskiĭ B I, Efros A L *Electronic Properties of Doped Semiconductors* (Berlin: Springer-Verlag, 1984)
36. Yafet Y, Keyes R W, Adams E N *Phys. Chem. Solids* **1** 137 (1956)
37. Polyakov D G *Zh. Eksp. Teor. Fiz.* **83** 546 (1982) [*Sov. Phys. JETP* **56** 33 (1982)]
38. Gor'kov L P, Dorokhov O N, Prigara F V *Zh. Eksp. Teor. Fiz.* **85** 582 (1983) [*Sov. Phys. JETP* **58** 852 (1983)]
39. Landau L D, Lifshitz E M *Quantum Mechanics* (Oxford: Pergamon, 1977)
40. Murzin S S *Pis'ma Zh. Eksp. Teor. Fiz.* **55** 665 (1992) [*JETP Lett.* **55** 696 (1992)]
41. Gogolin A A, Mel'nikov V I, Rashba É I *Zh. Eksp. Teor. Fiz.* **69** 328 (1975) [*Sov. Phys. JETP* **42** 168 (1975)]
42. Murzin S S, Jansen A G M, von der Linden P *Phys. Rev. Lett.* **80** 2681 (1998)
43. Murzin S S, Claus I, Jansen A G M *Pis'ma Zh. Eksp. Teor. Fiz.* **68** 305 (1998) [*JETP Lett.* **68** 327 (1998)]
44. Murzin S S et al. *Phys. Rev.* **59** 7330 (1999)
45. Halperin B I *Jpn. J. Appl. Phys. Suppl.* **26** 1913 (1987); in *Condensed Matter Theories* (Eds P Vashista et al.) (New York: Plenum, 1987)
46. Fortini A *Phys. Status Solidi B* **125** 259 (1984)
47. Kogan Sh M, Shadrin V D, Shul'man A Ya *Zh. Eksp. Teor. Fiz.* **68** 1377 (1975) [*Sov. Phys. JETP* **41** 686 (1975)]
48. Lax B et al. *Phys. Rev.* **122** 31 (1961)
49. Beckmann O, Hanamura E, Neuringer L J *Phys. Rev. Lett.* **18** 773 (1967)
50. Amirkhanov Kh I, Bashirov R I *Fiz. Tekh. Poluprovodn.* **1** 667 (1967)
51. Egorov F A, Murzin S S *Zh. Eksp. Teor. Fiz.* **94** 315 (1988) [*Sov. Phys. JETP* **67** 1045 (1988)]

52. Aronzon B A, Chumakov N K *Physica B* **194 – 196** 1165 (1994)
53. Murzin S S, Jansen A G M, Haanappel E G, to be published
54. Murzin S S, Popov P V *Pis'ma Zh. Eksp. Teor. Fiz.* **58** 280 (1993) [*JETP Lett.* **58** 289 (1993)]